Eur. J. Mineral., 32, 373–385, 2020
https://doi.org/10.5194/ejm-32-373-2020

European Journal of Mineralogy
Open Access

Niasite and johanngeorgenstadtite, $Ni^{2+}_{4.5}(AsO_4)_3$ dimorphs from Johanngeorgenstadt, Germany

Anthony R. Kampf[1], Barbara P. Nash[2], Jakub Plášil[3], Jason B. Smith[4], and Mark N. Feinglos[a,†]

[1]Mineral Sciences Department, Natural History Museum of Los Angeles County, 900 Exposition Boulevard, Los Angeles, CA 90007, USA
[2]Department of Geology and Geophysics, University of Utah, Salt Lake City, Utah 84112, USA
[3]Institute of Physics ASCR, v.v.i., Na Slovance 1999/2, 18221 Prague 8, Czech Republic
[4]2148 McClintock Rd., Charlotte, NC 28205, USA
[a]formerly at: Duke Medical Center, Durham, North Carolina 27710, USA
†deceased

Correspondence: Anthony R. Kampf (akampf@nhm.org)

Received: 31 March 2020 – Revised: 17 May 2020 – Accepted: 6 June 2020 – Published: 30 June 2020

Abstract. Niasite (IMA2019-105) and johanngeorgenstadtite (IMA2019-122) are $Ni^{2+}_{4.5}(AsO_4)_3$ dimorphs from Johanngeorgenstadt, Saxony, Germany. The two new minerals occur in association with one another and with aerugite, bunsenite, quartz, rooseveltite and xanthiosite. This mineral assemblage is apparently secondary in origin and most likely formed from the breakdown of primary nickeline under dry (low relative humidity) and oxidizing (high oxygen fugacity) conditions. Both minerals are found in sugary aggregates of irregular, rounded grains or short prisms. Niasite properties are as follows: colour violet-red to red-orange; streak pale pink; transparent; resinous to subadamantine lustre; brittle tenacity; no cleavage; conchoidal fracture; Mohs hardness ~ 4; density$_{calc}$ 5.222 g cm^{-3}; optically uniaxial (–), ω 1.925(5) and ε 1.855(5) (white light), pleochroism O beige, E deep pink ($O < E$). Johanngeorgenstadtite properties are as follows: colour pink-orange; streak pale pink; transparent; resinous to subadamantine lustre; brittle tenacity; {010}, {110} and {1 − 10} cleavage; curved and stepped fracture; Mohs hardness ~ 5; density$_{calc}$ 4.801 g cm^{-3}; optically biaxial (–), α 1.83(1), β 1.86(1), γ 1.88(1) (white light), $2V_{meas}$ 78(1)°, pleochroism X violet, Y light olive, Z yellow ($X > Y > Z$). Raman spectra of both minerals are dominated by the stretching vibrations of AsO_4 tetrahedra and confirm that both minerals are anhydrous. Electron microprobe analyses give the empirical formulas $(Ni^{2+}_{3.69}Co^{2+}_{0.66}Fe^{2+}_{0.03}Al_{0.02}Na_{0.02}Cu^{2+}_{0.01})_{\Sigma 4.43}As_{3.03}O_{12}$ and $(Ni^{2+}_{3.56}Co^{2+}_{0.75}Cu^{2+}_{0.13})_{\Sigma 4.44}As_{3.02}O_{12}$ for niasite and johanngeorgenstadtite, respectively. Niasite is tetragonal, $I\bar{4}2d$, with $a = 6.8046(8)$, $c = 18.6190(13)$ Å, $V = 862.1(2)$ Å^3 and $Z = 4$. Johanngeorgenstadtite is monoclinic, $C2/c$, with $a = 11.933(3)$, $b = 12.753(3)$, $c = 6.6956(17)$ Å, $\beta = 113.302(8)°$, $V = 935.9(4)$ Å^3 and $Z = 4$. The structure of niasite ($R_1 = 0.0226$ for 471 $I_o > 2\sigma I$ reflections) is the same as that of jeffbenite, as well as those of several garnet-like synthetic phases. Johanngeorgenstadtite ($R_1 = 0.0375$ for 355 $I_o > 2\sigma I$ reflections) has an unprotonated alluaudite structure.

1 Introduction

In their description of the new mineral paganoite, $NiBi^{3+}As^{5+}O_5$, Roberts et al. (2001) told the story of the enigmatic specimen on which it was discovered. This specimen was obtained by American mineral dealer David New in 1981 from a mineral shop in Germany but was without a label. In 1988, the late Mark N. Feinglos, who is also a co-author of the present paper, recognized the specimen to contain an unusual assemblage of minerals, including bunsenite, NiO, aerugite, $Ni_{17}As_6O_{32}$, and xanthiosite, $Ni_3(AsO_4)_2$, which is unique to one mineral locality, Johanngeorgenstadt, Saxony, Germany. (Note that the report of aerugite and xananthiosite from the South Terras mine,

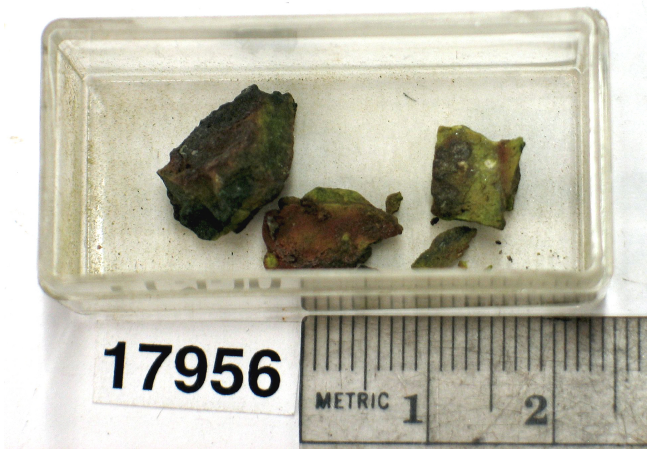

Figure 1. AMNH holotype specimen of johanngeorgenstadtite.

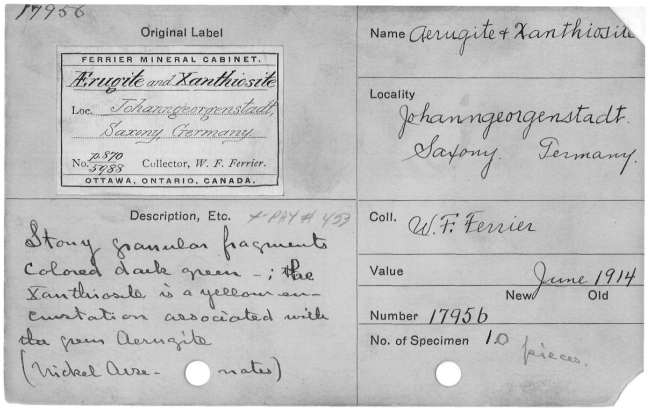

Figure 2. Old catalogue card with original Ferrier collection label for the AMNH holotype specimen of johanngeorgenstadtite.

Cornwall, England, by Davis et al. (1965) is now considered to be erroneous.) From this same specimen, Roberts et al. (2004) described the new mineral petewilliamsite, $(Ni, Co)_{30}(As_2O_7)_{15}$.

Subsequently, one of the authors of the present paper (JBS) obtained a sample thought to contain petewilliamsite; however, this mineral was actually determined to be niasite, one of the new minerals described herein. This sample was traced to the late James Ferriaolo, who is thought to have obtained it as surplus material from the American Museum of Natural History (AMNH). A search of Johanngeorgenstadt specimens in the AMNH collection turned up one specimen, no. 17956, consisting of three major fragments and numerous smaller ones (Fig. 1), which was subsequently found to also contain niasite. In a detailed examination of the minerals associated with niasite on the AMNH specimen, a second new mineral, johanngeorgenstadtite, was identified; this mineral is also described herein. The AMNH collection card and the original label (Fig. 2) indicate that the specimen, noted as including 10 pieces containing aerugite and xanthiosite, was obtained in June of 1914 from the collection of Walter F. Ferrier. It is likely that the fragment obtained by JBS was originally included among the fragments of this specimen. It should also be noted that pieces included in AMNH no. 17956 vary somewhat in appearance but are consistent in general mineralogy.

The name "niasite" is for the elements (not including oxygen) in the mineral's composition: nickel (Ni) + arsenic (As). The name "johanngeorgenstadtite" is for the locality, Johanngeorgenstadt, Germany. The minerals and their names have been approved by the IMA CNMNC (IMA2019-105 and IMA2019-122, respectively). The description of niasite is based upon on two cotype specimens. One cotype (measuring only a few millimetres in maximum dimension) is deposited in the collections of the Natural History Museum of Los Angeles County, 900 Exposition Boulevard, Los Angeles, CA 90007, USA, catalogue number 74203. The other cotype is in the collections of the American Museum of Natural History, Central Park West at 79th Street, New York City, NY 10024, USA, catalogue number 17956 (Figs. 1 and 2). The niasite cotype in the American Museum of Natural History collection is also the holotype for johanngeorgenstadtite.

2 Occurrence and associated minerals

As noted above, niasite and johanngeorgenstadtite were found on material from Johanngeorgenstadt, Saxony, Germany. Mining in Johanngeorgenstadt and the vicinity began in the second half of the 16th century but most probably took place during the 17th and 18th centuries. Besides silver, the major elements of interest were nickel and cobalt (based on the similarity to Jáchymov (Ondruš et al., 2003), which is less than 20 km SE, on the Bohemian side of the Erzgebirge). The discovery of anhydrous Ni and Co arsenates, such as those on the samples containing niasite and johanngeorgenstadtite, in the mid-19th century is probably related to the revived interest in nickel, cobalt and uranium for use in colouring glass. We were unable to find any specific information about this mining period. During the post-World War II Soviet era, the Wismut company worked the mines for uranium (Dietel, 2004; Bufka and Velebil, 2002).

Niasite and johanngeorgenstadtite are associated with aerugite, bunsenite, quartz, rooseveltite and xanthiosite. The association and general character of the samples are similar to the sample that yielded the new minerals paganoite (Roberts et al., 2001) and petewilliamsite (Roberts et al., 2004), although neither of these minerals was found in association with niasite and johanngeorgenstadtite. As noted for paganoite and petewilliamsite, the assemblage is apparently secondary in origin and most likely formed from the breakdown of primary nickeline under dry (low relative humidity, RH) and oxidizing (high oxygen fugacity) conditions.

The specimens that yielded niasite and johanngeorgenstadtite are quite small and, therefore, provide very limited paragenetic context; however, for comparison, the relatively large 7 cm × 5 cm × 4 cm holotype specimen for paganoite and petewilliamsite provides better context. The detailed description of this specimen by Roberts et al. (2001, 2004) and our own more recent observations on this specimen provide clear evidence that it was extracted from a natural vein and that it was not subjected to artificial processing following extraction. Roberts et al. (2001) note that

> The bulk of the specimen, which measures 7 × 5 × 4 cm, consists of a fine-grained quartz matrix with several veins of nickeline up to 4 mm thick, dispersed throughout. The nickeline veinlets are rimmed by native bismuth which, in turn, is rimmed by intergrown very dark-green crystals of bunsenite, up to 1 mm in size. Significant areas of the sample are richly covered by a number of colourful secondary minerals.

In addition, we noted a relatively fresh fracture on one side of the specimen, similar to what one would expect for a specimen extracted from a natural vein underground. We do not know exactly when these specimens were found, but aerugite and xanthiosite were described in 1858 (Bergemann, 1858). We note that, at about that same time, extensive reopening of old workings had been undertaken in the neighbouring Jáchymov mining district (see e.g. Vogl, 1856). We consider it likely that the unique mineral assemblage comprising aerugite, xanthiosite, bunsenite, paganoite, petewilliamsite, and niasite and johanngeorgenstadtite, described herein, was encountered during reopening of old stopes that date to the first half of the 17th century.

It is worth noting that during this earlier mining period, the practice of fire-setting was still in use in the Jáchymov ore district and probably also at Johanngeorgenstadt. We cannot discount the possibility that fire-setting was a factor in the alteration of the vein that yielded this anhydrous supergene mineral assemblage. Barbier (1999) crystallized the synthetic equivalent of niasite by heating $Ni_3As_2O_8{\cdot}8H_2O$ (synthetic annabergite) at 750 °C and 1 kbar in a cold-seal hydrothermal reactor for 6 d. He also synthesized microcrystalline material by heating powdered $Ni_3As_2O_8{\cdot}8H_2O$ to 750–800 °C in air. In a paper discussing fire-setting, Weisgerber and Willies (2000) report that temperatures over 700 °C can be readily sustained for considerable periods using wood fires, and working temperatures up to 800 °C ought to be achievable.

The secondary phases occur in granular intergrowths and we observed no straightforward clues for deciphering a paragenetic sequence for these phases. It appears that they formed roughly contemporaneously. According to the Ostwald–Volmer rule for metastable crystallization (Holleman et al., 2001), the less dense phase forms first because, under supersaturation conditions, its nuclei reach critical size faster than those of the more dense phase (Fischer and Jansen, 2002; Bach et al., 2013). Considering that johanngeorgenstadtite is less dense than niasite (4.801 vs 5.222 g cm^{-3}), it would be expected to precede niasite in the paragenetic sequence; however, such a sequence cannot be confirmed from observations on the crystal intergrowths.

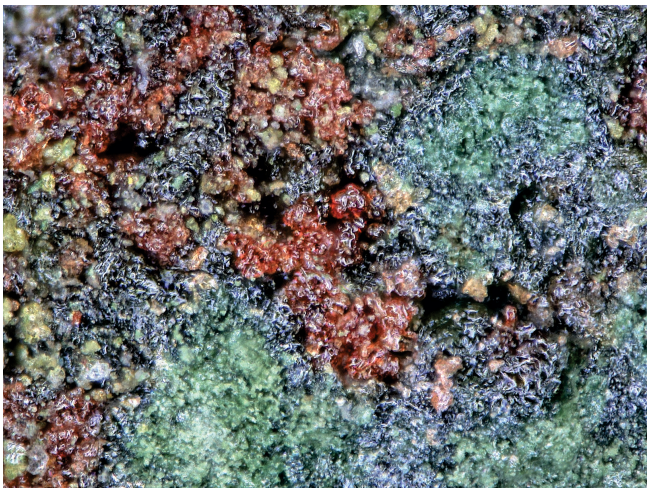

Figure 3. Niasite (red) with aerugite (green) and xanthiosite (yellow) on cotype specimen (LACMNH 74203); FOV 0.56 mm across.

3 Physical and optical properties

3.1 Niasite

Niasite occurs in sugary aggregates of violet-red to red-orange irregular, rounded grains or short prisms that are about 50 µm in diameter (Fig. 3). No forms could be determined and no twinning was observed. The streak is pale pink. Crystals are transparent with resinous to subadamantine lustre. No fluorescence was observed in long- or short-wave ultraviolet illumination. Scratch tests provided a Mohs hardness of about 4. Crystals are brittle with conchoidal fracture and no cleavage. The calculated density is 5.222 g cm^{-3} for the empirical formula and 5.245 g cm^{-3} for the ideal formulas, in both cases based on the single-crystal cell. At room temperature, niasite is insoluble in concentrated HCl and concentrated H_2SO_4.

Optically, niasite is uniaxial (–), with the indices of refraction $\omega = 1.925(5)$ and $\varepsilon = 1.855(5)$, measured in white light. The mineral is distinctly pleochroic with O beige, E deep pink; $O < E$. The Gladstone–Dale compatibility, $1 - (K_P/K_C)$, (Mandarino, 1981) is −0.021 (excellent) for the empirical formula and −0.017 (superior) for the ideal formula, in both cases using the single-crystal cell.

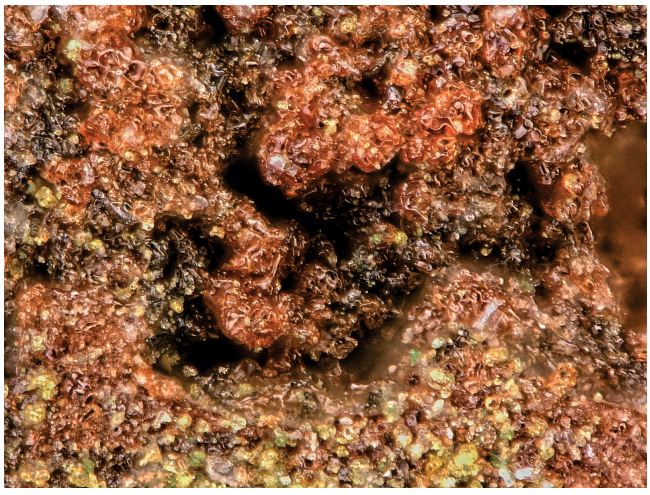

Figure 4. Johanngeorgenstadtite (pink orange) with aerugite (green) and xanthiosite (yellow) on holotype specimen (AMNH 17956); FOV 0.56 mm across.

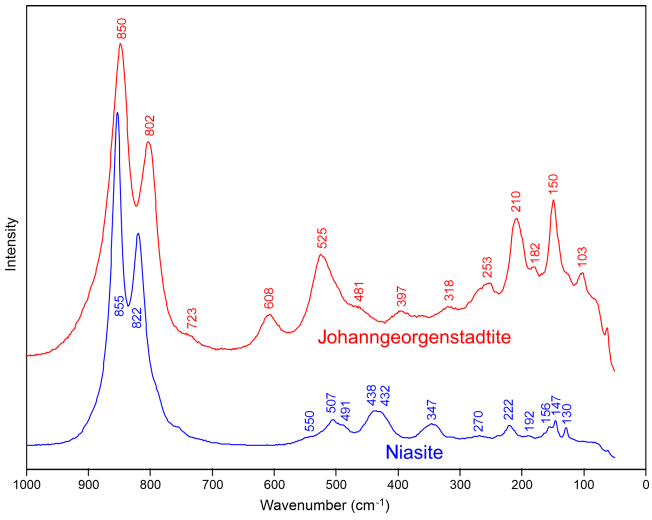

Figure 5. Raman spectra of johanngeorgenstadtite and niasite recorded using a 532 nm laser.

3.2 Johanngeorgenstadtite

Johanngeorgenstadtite occurs in sugary aggregates of pink-orange irregular, rounded grains or short prisms that are about 70 µm in diameter (Fig. 4). No forms could be determined and no twinning was observed. The streak is pale pink. Crystals are transparent with resinous to subadamantine lustre. No fluorescence was observed in long- or short-wave ultraviolet illumination. Scratch tests to determine the Mohs hardness were inconclusive; however, based on the difficulty in breaking small grains, the mineral is estimated to have a hardness of about 5. Crystals are brittle with curved and stepped fracture. Multiple cleavage planes are apparent and these probably correspond to {010}, {110} and $\{1\bar{1}0\}$, by analogy with other alluaudite-group minerals. The calculated density is 4.801 g cm^{-3} for the empirical formula and 4.808 g cm^{-3} for the ideal formula, in both cases based on the single-crystal cell. In dilute HCl at room temperature, johanngeorgenstadtite rapidly loses colour (indicating decomposition) and slowly dissolves.

Optically, johanngeorgenstadtite is biaxial (–), with the indices of refraction $\alpha = 1.83(1)$, $\beta = 1.86(1)$ and $\gamma = 1.88(1)$, measured in white light. A measured $2V$ of 78(1)° was obtained from extinction data using EXCALIBRW (Gunter et al., 2004). The calculated $2V$ is 77.3°. Dispersion could not be observed and the optical orientation could not be determined. The mineral is distinctly pleochroic with X violet, Y light olive, Z yellow; $X > Y > Z$. The Gladstone–Dale compatibility, $1 - (K_P/K_C)$, (Mandarino, 1981) is −0.056 (good) for the empirical formula and −0.055 (good) for the ideal formula. The small size and irregular shape of crystal grains coupled with relatively high indices of refraction made the determination of the optical properties particularly challenging. This, in part, may account for the only good Gladstone–Dale compatibility.

4 Raman spectroscopy

Raman spectroscopy was done on a Horiba XploRa+ micro-Raman spectrometer using an incident wavelength of 532 nm, laser slit of 50 µm, 2400 gr mm^{-1} diffraction grating and a 100x (0.9 NA) objective. Spectra for niasite and johanngeorgenstadtite were recorded from 4000 to 60 cm^{-1} but were featureless from 4000 to 1000 cm^{-1}. The spectra from 1000 to 60 cm^{-1} are shown in Fig. 5.

The Raman spectra of both minerals are dominated by the stretching vibrations of AsO_4 tetrahedra. There are no apparent bands in the regions of O–H stretching or (δ) H–O–H deformation of H_2O. The overlapping composite band (doublet) of highest intensity, composed of bands at 855 and 822 cm^{-1} for niasite and 850 and 802 cm^{-1} for johanngeorgenstadtite, is attributed to overlapping ν_3 antisymmetric and ν_1 symmetric As–O vibrations of the AsO_4 tetrahedra. Other spectral features differ significantly between the two minerals.

For niasite, bands of lower intensity at ∼ 550, 507 and 491 cm^{-1} are related to the ν_4 (δ) AsO_4 tetrahedra. At least two of the overlapping bands of medium weak intensity at 438 and 432 cm^{-1} are related to the ν_2 (δ) AsO_4 bending vibrations. The composite band at ∼ 347 cm^{-1} may be related to the stretching vibrations of the $Ni3O_4$ polyhedra. Bands observed at the lowest energies (270, 222, 192, 156, 147 and 130 cm^{-1}) are related to various M–O_x stretching vibrations and/or to phonons.

For johanngeorgenstadtite, the rather broad bands at 608 and 525 cm^{-1} (with shoulders towards lower energies) are re-

Table 1. Analytical data (wt %) for niasite and johanngeorgenstadtite.

	Niasite			Johanngeorgenstadtite			
Constituent	Mean	Range	SD	Mean	Range	SD	Standard
Na_2O	0.08	0.00–0.20	0.10	BDL	–	–	albite
Ag_2O	0.06	0.00–0.15	0.07	BDL	–	–	Ag metal
FeO	0.29	0.12–0.56	0.21	BDL	–	–	hematite
NiO	40.38	36.91–43.79	3.10	39.12	38.71–39.60	0.34	Ni metal
CoO	7.26	5.42–8.54	1.39	8.23	7.84–8.52	0.28	Co metal
CuO	0.13	0.07–0.19	0.04	1.54	1.47–1.61	0.05	Cu metal
Al_2O_3	0.15	0.01–0.35	0.17	BDL	–	–	albite
As_2O_5	51.03	50.27–51.58	0.48	51.12	49.74–52.12	0.94	GaAs
Total	99.38			100.01			

BDL denotes "below detection limit".

lated to the split ν_4 (δ) of AsO_4 tetrahedra. The low-intensity bands at 481 and 397 cm^{-1} are probably related to the ν_2 (δ) AsO_4 bending vibrations. The low-intensity composite band at $\sim 318\,cm^{-1}$ may be related to the Ni–O stretching vibrations. Bands observed at the lowest energies (253, 210, 182, 150 and 103 cm^{-1}) are related to various M–O_x stretching vibrations and/or to phonons.

5 Chemical compositions

Analyses (five points on four crystals for each mineral) were performed at the University of Utah on a Cameca SX-50 electron microprobe with four wavelength dispersive spectrometers and using Probe for EPMA software. Analytical conditions were 15 kV accelerating voltage, 20 nA beam current and 5 µm beam diameter. Raw X-ray intensities were corrected for matrix effects with a $\varphi\rho(z)$ algorithm (Pouchou and Pichoir, 1991). No other elements were detected by energy dispersive spectroscopy (EDS) or by wavelength dispersive spectroscopy (WDS) wave scans. The lack of any O–H features in the Raman spectra confirmed the phases to be anhydrous. There was no damage from the electron beam. The analytical results are provided in Table 1.

For niasite, the empirical formula based on 12 O atoms per formula unit (apfu) is $(Ni^{2+}_{3.69}Co^{2+}_{0.66}Fe^{2+}_{0.03}Al_{0.02}Na_{0.02}Cu^{2+}_{0.01})_{\Sigma 4.43}As_{3.03}O_{12}$ and the simplified formula is $(Ni^{2+}, Co^{2+}, Fe^{2+}, Al, Na, Cu^{2+})_{4.5}(AsO_4)_3$. For johanngeorgenstadtite, the empirical formula based on 12 O apfu is $(Ni^{2+}_{3.56}Co^{2+}_{0.75}Cu^{2+}_{0.13})_{\Sigma 4.44}As_{3.02}O_{12}$ and the simplified formula is $(Ni^{2+}, Co^{2+}, Cu^{2+})_{4.5}(AsO_4)_3$. Only considering major substitutions, both minerals have the same simplified formula, $(Ni^{2+},Co^{2+})_{4.5}(AsO_4)_3$. Both minerals also have the same ideal formula, $Ni^{2+}_{4.5}(AsO_4)_3$, which requires NiO 49.37, As_2O_5 50.63 and total 100 wt %.

Niasite Ni^{2+} and Co^{2+} analyses varied over relatively wide ranges and exhibited a negative correlation, indicative of substitution of one for the other, as is common for these cations. There was relatively little variation in the Ni^{2+} and Co^{2+} analyses for johanngeorgenstadtite; however, considering the limited number of analyses, this should not be construed as indicative of more limited $Ni^{2+} \leftrightarrow Co^{2+}$ substitution in johanngeorgenstadtite.

6 X-ray crystallography and crystal structure determinations

X-ray powder diffraction data were recorded on a Rigaku R-Axis Rapid II curved imaging plate microdiffractometer with monochromatized MoKα radiation. A Gandolfi-like motion on the φ and ω axes was used to randomize the polycrystalline samples. Observed d values and intensities were derived by profile fitting using JADE 2010 software (Materials Data, Inc.). Data (in ångströms) for niasite and johanngeorgenstatite are given in Table 2a and b, respectively.

Single-crystal X-ray studies were carried out using the same diffractometer and radiation used for the powder studies. The Rigaku CrystalClear software package was used for processing the structure data, including the application of empirical absorption corrections using the multi-scan method with ABSCOR (Higashi, 2001). The structures were solved by the charge-flipping method using SHELXT (Sheldrick, 2015a). Refinements proceeded with full-matrix least squares on F^2 using SHELXL-2016 (Sheldrick, 2015b). The niasite and johanngeorgenstadtite crystals used for the data collections were similarly small in size, 35 µm × 30 µm × 20 µm and 40 µm × 30 µm × 20 µm, respectively; however, niasite proved to diffract X-rays much more effectively than johanngeorgenstadtite, presumably because of its densely packed structure (see below). Data were collected for niasite to $2\theta \approx 55°$, while those for johanngeorgenstadtite were limited to $2\theta < 40°$. The latter provided a low data-to-parameter ratio; however, the structure refinement for johanngeorgenstadtite was well behaved and pro-

Table 2. **(a)** Powder X-ray data (d in ångströms) for niasite. Only calculated lines with $I \geq 2$ are listed. **(b)** Powder X-ray data (d in ångströms) for johanngeorgenstadtite*. Only calculated lines with $I \geq 2$ after factoring are listed.

(a)				
I_{obs}	d_{obs}	d_{calc}	I_{calc}	$h\ k\ l$
		6.3912	2	1 0 1
9	4.644	4.6548	5	0 0 4
		4.5855	6	1 0 3
4	4.313	4.2744	2	1 1 2
18	3.274	3.2666	21	1 0 5
2	3.187	3.1956	3	2 0 2
25	3.008	3.0033	27	2 1 1
100	2.752	2.7468	100	2 0 4
		2.7323	8	2 1 3
9	2.408	2.4058	12	2 2 0
10	2.330	2.3564	2	2 1 5
		2.3274	11	0 0 8
2	2.257	2.2927	3	2 0 6
		2.2516	2	3 0 1
4	2.141	2.1304	2	3 0 3
4	2.101	2.0965	5	3 1 2
4	1.999	2.0027	2	2 1 7
4	1.943	1.9532	2	3 1 4
		1.9209	2	2 0 8
4	1.880	1.8776	4	3 2 1
3	1.808	1.8056	3	3 2 3
3	1.772	1.7683	4	3 1 6
21	1.706	1.7109	10	2 1 9
		1.7012	15	4 0 0
28	1.678	1.6834	12	3 2 5
		1.6734	2	4 0 2
		1.6727	19	2 2 8
4	1.583	1.5806	5	3 3 2
4	1.549	1.5516	2	0 0 12
9	1.533	1.5392	5	3 2 7
		1.5285	5	3 0 9
		1.5216	2	4 2 0
7	1.509	1.5088	6	4 1 5
2	1.490	1.4792	2	2 1 11
13	1.446	1.4462	14	4 2 4
10	1.412	1.4248	4	3 3 6
		1.4117	7	2 0 12
		1.4080	2	3 1 10
		1.4015	3	1 0 13
6	1.368	1.3734	5	4 0 8
		1.3662	3	4 2 6

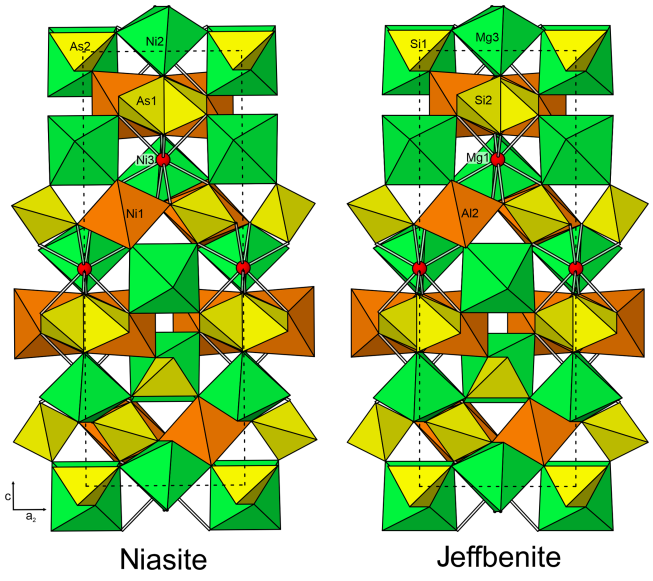

Figure 6. Crystal structures of niasite and jeffbenite. Note that the jeffbenite cell has been shifted by one-half along c to correspond to the niasite cell.

vided a structure entirely consistent with the unprotonated alluaudite structure type.

The data collection and refinement details for niasite and johanngeorgenstadtite are given in Table 3, atom coordinates and displacement parameters in Table 4a and b, selected bond distances in Table 5a and b, and bond-valence sums (BVS) in Table 6a and b.

7 Descriptions of the crystal structures

7.1 Niasite

Niasite is isostructural with synthetic $Ni_{4.35}As_3O_{11.7}(OH)_{0.3}$ (Barbier, 1999), as well as with the garnet-like structure of a variety of phases (see Lévy and Barbier, 2000). These include the synthetic phases $Co_{4.5}(AsO_4)_3$ (Gopal et al., 1980), $Mg_{4.5}(AsO_4)_3$ (Krishnachari and Calvo, 1973), $NaMg_4(AsO_4)_3$ (Murashova et al., 1988) and $(Mg,Fe)_{0.85}(Mg,Fe)_4(Fe,Ge)_3O_{12}$ (Lévy and Barbier, 2000) and the mineral jeffbenite, $Mg_3Al_2Si_3O_{12}$ (Nestola et al., 2016; Finger and Conrad, 2000). Each of these structures includes two tetrahedra, two octahedra and one dodecahedron that are connected by corner and edge sharing to form a dense framework, which is not based on a close-packed array of O atoms. The structure of niasite is compared with that of jeffbenite (translated by one-half along c) in Fig. 6.

In the niasite structure, the two tetrahedrally coordinated cation sites (As1 and As2) are both fully occupied by As, the two octahedrally coordinated cation sites (Ni1 and Ni2) are both fully occupied jointly by Ni and Co, and the dodecahedrally coordinated site (Ni3) is partially occupied. Although

Table 2. Continued.

(b)

I_{obs}	d_{obs}	d_{calc}	I_{calc}	$h\ k\ l$	I_{obs}	d_{obs}	d_{calc}	I_{calc}	$h\ k\ l$
9	6.337	6.377	8	0 2 0	17	1.948	1.948	3	5 3 0
8	4.074	4.054	3	$\bar{2}$ 2 1			1.946	9	$\bar{3}$ 5 2
		3.719	2	$\bar{3}$ 1 1	5	1.865	1.875	2	2 4 2
		3.572	4	$\bar{1}$ 3 1	6	1.847	1.853	7	1 5 2
16	3.514	3.512	13	3 1 0			1.828	2	$\bar{2}$ 4 3
		3.295	5	$\bar{2}$ 0 2	4	1.809	1.806	2	3 3 2
48	3.215	3.215	53	$\bar{1}$ 1 2	5	1.750	1.756	4	$\bar{1}$ 7 1
		3.134	5	1 3 1	28	1.661	1.661	13	$\bar{2}$ 0 4
18	3.076	3.075	15	0 0 2			1.660	11	$\bar{6}$ 4 2
		3.046	4	2 2 1			1.594	2	0 8 0
		2.931	3	$\bar{3}$ 1 2	16	1.585	1.585	9	6 4 0
7	2.831	2.831	7	0 4 1	4	1.552	1.559	2	$\bar{3}$ 7 2
100	2.748	2.771	6	3 3 0			1.554	2	7 1 0
		2.756	65	2 4 0			1.525	2	$\bar{2}$ 8 1
		2.740	29	4 0 0	8	1.525	1.523	5	4 4 2
		2.638	2	1 1 2	13	1.510	1.511	4	3 7 1
20	2.623	2.626	15	$\bar{4}$ 0 2			1.510	2	1 7 2
		2.618	8	$\bar{1}$ 3 2			1.507	2	2 4 3
4	2.454	2.457	5	$\bar{3}$ 3 2			1.506	3	$\bar{6}$ 0 4
4	2.312	2.319	5	2 0 2	7	1.489	1.489	5	$\bar{8}$ 0 2
5	2.288	2.291	6	$\bar{2}$ 4 2			1.469	2	7 3 0
		2.277	2	1 3 2	9	1.462	1.464	7	$\bar{4}$ 4 4
4	2.214	2.221	4	$\bar{5}$ 1 2	10	1.404	1.410	3	$\bar{7}$ 5 2
		2.213	2	0 4 2			1.397	3	$\bar{1}$ 7 3
		2.177	2	$\bar{4}$ 4 1	10	1.383	1.385	6	0 4 4
8	2.162	2.160	4	5 1 0			1.370	2	8 0 0
		2.126	2	0 6 0	8	1.350	1.353	2	6 0 2
6	2.088	2.091	3	3 5 0			1.348	5	2 0 4
2	2.017	2.027	2	$\bar{4}$ 4 2	4	1.322	1.323	3	$\bar{5}$ 7 3
6	1.981	1.993	2	$\bar{5}$ 3 2	6	1.306	1.307	2	5 5 2
		1.972	5	3 1 2			1.303	2	$\bar{1}$ 9 2
		1.951	2	$\bar{3}$ 3 3					

* Calculated intensities have been factored so that the three lines contributing to the peak of highest observed intensity have an aggregate intensity of 100.

Table 3. Data collection and refinement conditions for niasite and johanngeorgenstadtite.

Diffractometer	Rigaku R-Axis Rapid II	
X-ray radiation	MoKα ($\lambda = 0.71075$ Å)	
Temperature	293(2) K	
Refined cell contents ($\times 1/4$)	$Ni_{4.10}(AsO_4)_3$	$Ni_{4.61}(AsO_4)_3$
Space group	I-42d (#122)	$C2/c$ (#15)
Unit cell dimensions	$a = 6.8046(8)$ Å $c = 18.6190(13)$ Å	$a = 11.933(3)$ Å $b = 12.753(3)$ Å $c = 6.6956(17)$ Å $\beta = 113.302(8)°$
V	862.1(2) Å^3	935.9(4) Å^3
Z	4	4
Density (for above formula)	5.065 g cm^{-3}	4.880 g cm^{-3}
Absorption coefficient	20.316 mm^{-1}	19.716 mm^{-1}
$F(000)$	1239.2	1296.6
Crystal size	35 mm × 30 mm × 20 mm	40 mm × 30 mm × 20 mm
θ range	3.19 to 27.34°	3.20 to 19.96°
Index ranges	$-6 \le h \le 8$ $-6 \le k \le 8$ $-22 \le l \le 21$	$-11 \le h \le 11$ $-11 \le k \le 12$ $-6 \le l \le 6$
Refls collected/unique	1831/499; $R_{int} = 0.052$	1868/438; $R_{int} = 0.086$
Reflections with $I_o > 2\sigma I$	471	355
Completeness to θ_{max}	99.6 %	99.5 %
Refinement method	Full-matrix least squares on F^2	
Parameters/restraints	51/0	104/0
GoF	1.089	1.067
Final R indices [$I_o > 2\sigma I$]	$R_1 = 0.0226$, $wR_2 = 0.0442$	$R_1 = 0.0375$, $wR_2 = 0.0869$
R indices (all data)	$R_1 = 0.0246$, $wR_2 = 0.0446$	$R_1 = 0.0494$, $wR_2 = 0.0957$
Absolute structure parameter	0.03(3)	
Extinction coefficient	0.00012(16)	0
Largest diff. peak/hole	$+0.79/-1.11e$/Å^3	$+0.74/-0.79e$/Å^3

$R_{int} = \Sigma|F_o^2 - F_o^2(\text{mean})|/\Sigma[F_o^2]$. GoF $= S = \{\Sigma[w(F_o^2 - F_c^2)^2]/(n-p)\}^{1/2}$. $R_1 = \Sigma||Fo| - |Fc||/\Sigma|Fo|$. $wR_2 = \{\Sigma[w(F_o^2 - F_c^2)^2]/\Sigma[w(F_o^2)^2]\}^{1/2}$; $w = 1/[\sigma^2(F_o^2) + (aP)^2 + bP]$, where a is 0.0178 (niasite) and 0.053 (johanngeorgenstadtite), b is 0, and P is $[2F_c^2 + \text{Max}(F_o^2, 0)]/3$.

scattering powers of Ni and Co are too similar to allow refinement of their relative occupancies in the Ni1 and Ni2 sites with high confidence, the refinement does suggest that (1) these sites are essentially fully occupied by Ni and Co, (2) neither site is strongly preferred by either cation over the other, and (3) Ni is clearly dominant in both sites.

As has been noted in all previous reports on this structure type, the dodecahedrally eight-coordinated site (Fig. 7) is particularly noteworthy. It includes four shorter bonds (2.209 Å in niasite) and four longer bonds (2.707 Å in niasite). As noted by Lévy and Barbier (2000), the dodecahedral site is ideally half occupied in the arsenates with this structure, while in other phases, such as jeffbenite,

Table 4. (a) Atom coordinates and displacement parameters (Å^2) for niasite. **(b)** Atom coordinates and displacement parameters (Å^2) for johanngeorgenstadtite.

(a)	x/a	y/b	z/c	U_{eq}		Occupancy
Ni1	0.7522(3)	1/4	1/8	0.0068(4)		$Ni_{0.983(6)}$
Ni2	0	1/2	0.2291(7)	0.0069(4)		$Ni_{0.971(5)}$
Ni3	0	1/2	3/4	0.013(3)		$Ni_{0.200(7)}$
As1	0.34532(14)	1/4	1/8	0.0059(3)		1
As2	0	1/2	1/4	0.0051(7)		1
O1	0.9445(7)	0.2905(7)	0.2059(2)	0.0094(12)		1
O2	0.5094(7)	0.2856(7)	0.1937(2)	0.0102(12)		1
O3	0.2225(7)	0.0449(6)	0.1471(2)	0.0084(10)		1
	U^{11}	U^{22}	U^{33}	U^{23}	U^{13}	U^{12}
Ni1	0.0060(6)	0.0064(6)	0.0082(7)	−0.0003(5)	0	0
Ni2	0.0065(7)	0.0067(7)	0.0074(6)	0	0	−0.0009(6)
Ni3	0.011(4)	0.011(4)	0.017(5)	0	0	0
As1	0.0057(5)	0.0046(5)	0.0074(5)	−0.0005(4)	0	0
As2	0.0042(5)	0.0042(5)	0.0070(6)	0	0	0
O1	0.016(3)	0.003(3)	0.009(2)	−0.0013(18)	−0.0046(19)	−0.001(2)
O2	0.007(2)	0.014(3)	0.009(2)	−0.0045(19)	−0.0032(19)	0.002(2)
O3	0.008(3)	0.007(2)	0.010(2)	−0.0001(17)	0.0037(18)	−0.003(2)
(b)	x/a	y/b	z/c	U_{eq}	Occupancy	
$A1'$	0	0.50304(19)	0.25	0.0213(15)	1.000(12) Ni	
$A2$	0	0	0	0.045(5)	0.322(13) Ni	
$A2'$	0	−0.0078(5)	0.25	0.026(3)	0.464(12) Ni	
$M1$	0	0.2562(2)	0.25	0.0234(14)	0.941(9) Ni	
$M2$	0.28491(19)	0.65782(16)	0.3752(3)	0.0247(10)	0.943(7) Ni	
As1	0	−0.28590(17)	0.25	0.0231(8)	1	
As2	0.23274(15)	−0.11382(11)	0.1264(2)	0.0230(7)	1	
O1	0.4635(9)	0.7125(7)	0.5232(14)	0.025(2)	1	
O2	0.1063(9)	0.6204(7)	0.2612(15)	0.024(3)	1	
O3	0.3394(8)	0.6718(7)	0.1202(13)	0.027(3)	1	
O4	0.1160(9)	0.3923(7)	0.3123(15)	0.031(3)	1	
O5	0.2167(8)	0.8111(7)	0.3211(13)	0.026(3)	1	
O6	0.3298(10)	0.5037(7)	0.3850(17)	0.032(3)	1	
	U^{11}	U^{22}	U^{33}	U^{23}	U^{13}	U^{12}
$A1'$	0.024(2)	0.022(2)	0.018(2)	0	0.0086(16)	0
$A2$	0.041(9)	0.032(7)	0.063(9)	−0.007(5)	0.023(7)	−0.009(5)
$A2'$	0.027(5)	0.033(5)	0.019(4)	0	0.008(4)	0
$M1$	0.024(2)	0.031(2)	0.017(2)	0	0.0100(17)	0
$M2$	0.0315(17)	0.0268(15)	0.0191(14)	0.0002(10)	0.0136(12)	0.0000(11)
As1	0.0309(17)	0.0251(14)	0.0147(13)	0	0.0105(12)	0
As2	0.0274(12)	0.0252(11)	0.0172(10)	−0.0012(8)	0.0098(9)	-0.0019(8)
O1	0.038(7)	0.021(6)	0.020(5)	−0.013(5)	0.017(5)	−0.006(5)
O2	0.025(6)	0.024(6)	0.028(5)	−0.001(5)	0.015(5)	−0.006(5)
O3	0.036(7)	0.033(7)	0.011(5)	−0.002(5)	0.010(5)	−0.007(5)
O4	0.023(6)	0.037(7)	0.033(6)	0.001(5)	0.012(5)	0.000(5)
O5	0.032(7)	0.029(6)	0.017(5)	0.006(5)	0.011(5)	0.012(5)
O6	0.033(8)	0.026(6)	0.041(6)	0.005(5)	0.017(6)	−0.007(5)

Table 5. (a) Selected bond distances (Å) for niasite. **(b)** Selected bond distances (Å) for johanngeorgenstadtite.

(a)					
Ni1–O1 (×2)	2.014(4)	Ni3–O2 (×4)	2.209(5)		
Ni1–O3 (×2)	2.056(4)	Ni3–O3 (×4)	2.707(4)		
Ni1–O2 (×2)	2.103(4)	⟨ Ni3–O ⟩	2.458		
⟨ Ni1–O ⟩	2.058				
		As1–O3 (×2)	1.678(4)		
Ni2–O1 (×2)	2.051(5)	As1–O2 (×2)	1.714(4)		
Ni2–O2 (×2)	2.076(5)	⟨ As1–O ⟩	1.696		
Ni2–O3 (×2)	2.145(4)				
⟨ Ni2–O ⟩	2.091	As2–O1 (×4)	1.688(4)		
(b)					
*M*1–O3 (×2)	2.067(9)	*A*1′–O4 (×2)	1.904(10)	As1–O1 (×2)	1.688(8)
*M*1–O1 (×2)	2.116(9)	*A*1′–O2 (×2)	1.945(9)	As1–O2 (×2)	1.723(9)
*M*1–O4 (×2)	2.155(10)	⟨ *A*1′–O ⟩	1.925	⟨ As1–O ⟩	1.706
⟨ *M*1–O4 ⟩	2.113				
		*A*2–O6 (×2)	1.866(11)	As2–O6	1.662(9)
*M*2–O2	2.016(9)	*A*2–O1 (×2)	2.759(9)	As2–O4	1.688(10)
*M*2–O6	2.032(9)	*A*2–O3 (×2)	3.216(9)	As2–O5	1.689(9)
*M*2–O3	2.061(8)	*A*2–O3 (×2)	3.329(9)	As2–O3	1.699(9)
*M*2–O5	2.079(8)	⟨ *A*2–O ⟩	2.793	⟨ As2–O ⟩	1.685
*M*2–O1	2.083(10)				
*M*2–O5	2.094(9)	*A*2′–O6 (×2)	2.485(11)		
⟨ *M*2–O4 ⟩	2.061	*A*2′–O6 (×2)	2.533(10)		
		*A*2′–O3 (×2)	2.890(11)		
		*A*2′–O1 (×2)	2.965(10)		
		⟨ *A*2′–O ⟩	2.718		

it can be close to fully occupied. Also of note is that the BVS values for the dodecahedrally coordinated divalent cations in the arsenates are always very low (0.70 vu in $Ni_{4.35}As_3O_{11.7}(OH)_{0.3}$ and 1.08 vu in niasite). Barbier (1999) found less than ideal half occupancy of the dodecahedral site in $Ni_{4.35}As_3O_{11.7}(OH)_{0.3}$ and suggested that charge balance is achieved by substitution of OH for some O, although no proof for the presence of OH was provided. We found no evidence for OH in the Raman spectrum of niasite, but that does not necessarily prove that a small amount of OH is not present.

The low refined occupancy of the Ni3 site is actually somewhat higher considering likely minor occupancy by cations with lower scattering power than Ni, such as Na. In addition, the low bond-valence sums (BVS) for the coordinated O2 and O3 sites are improved to nearly ideal values by a total occupancy of 0.5 for the Ni3 site. It may be that the apparent low occupancy of the Ni3 site is, at least in part, an artefact of the refinement. In any case, considering the EPMA evidence for niasite and evidence from previous studies of analogous phases, we conclude that the ideal formula for niasite is best given as $Ni^{2+}_{4.5}(AsO_4)_3$.

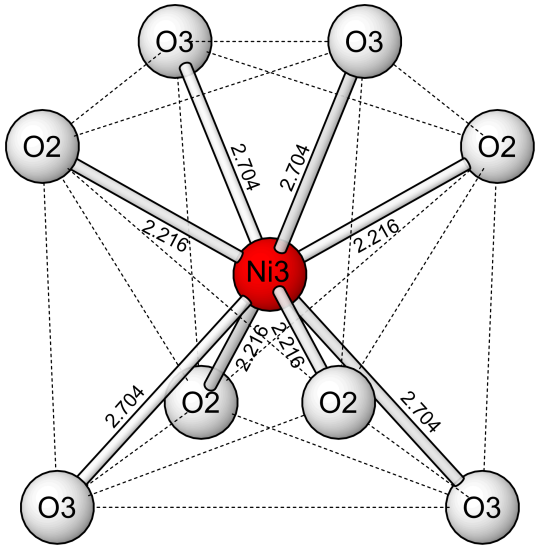

Figure 7. The dodecahedrally coordinated site in the structure of niasite.

Table 6. (a) Bond-valence analysis for niasite. Values are expressed in valence units (vu). **(b)** Bond-valence analysis for johanngeorgenstadtite. Values are expressed in valence units (vu).

(a)	Ni1	Ni2	Ni3	As1	As2	Sum
O1	$0.39^{\times 2\downarrow}$	$0.35^{\times 2\downarrow}$			$1.24^{\times 4\downarrow}$	1.99
O2	$0.30^{\times 2\downarrow}$	$0.33^{\times 2\downarrow}$	$0.22^{\times 4\downarrow 0.2\rightarrow}$	$1.16^{\times 2\downarrow}$		1.84
O3	$0.35^{\times 2\downarrow}$	$0.27^{\times 2\downarrow}$	$0.05^{\times 4\downarrow 0.2\rightarrow}$	$1.28^{\times 2\downarrow}$		1.91
Sum	2.08	1.90	1.08	4.88	4.96	

(b)	$A1'$	$A2$	$A2'$	$M1$	$M2$	As1	As2	Sum
O1		$0.05^{\times 2\downarrow}$ $\times 0.322\rightarrow$	$0.03^{\times 2\downarrow}$ $\times 0.464\rightarrow$	$0.29^{\times 2\downarrow}$	0.32	$1.24^{\times 2\downarrow}$		1.87
O2	$0.48^{\times 2\downarrow}$				0.39	$1.13^{\times 2\downarrow}$		2.00
O3		$0.01^{\times 4\downarrow}$ $\times 0.322\rightarrow$	$0.03^{\times 2\downarrow}$ $\times 0.464\rightarrow$	$0.34^{\times 2\downarrow}$	0.34		1.21	1.90
O4	$0.54^{\times 2\downarrow}$			$0.26^{\times 2\downarrow}$			1.24	2.04
O5					0.33 0.31		1.24	1.88
O6		$0.60^{\times 2\downarrow}$ $\times 0.322\rightarrow$	$0.10^{\times 2\downarrow}$ $\times 0.464\rightarrow$ $0.09^{\times 2\downarrow}$ $\times 0.464\rightarrow$		0.37		1.34	1.99
Sum	2.04	1.32	0.50	1.78	2.06	4.74	5.03	

Multiplicities indicated by $\times\downarrow\rightarrow$; Ni1 and Ni2 sites are taken as fully occupied by Ni. The $M1$, $M2$, $A1'$, $A2$ and $A2'$ sites are assigned only as Ni, with full occupancies being used for the $M1$, $M2$ and $A1'$ sites and refined occupancies being used for the $A2$ and $A2'$ sites. Bond-valence parameters are from Gagné and Hawthorne (2015).

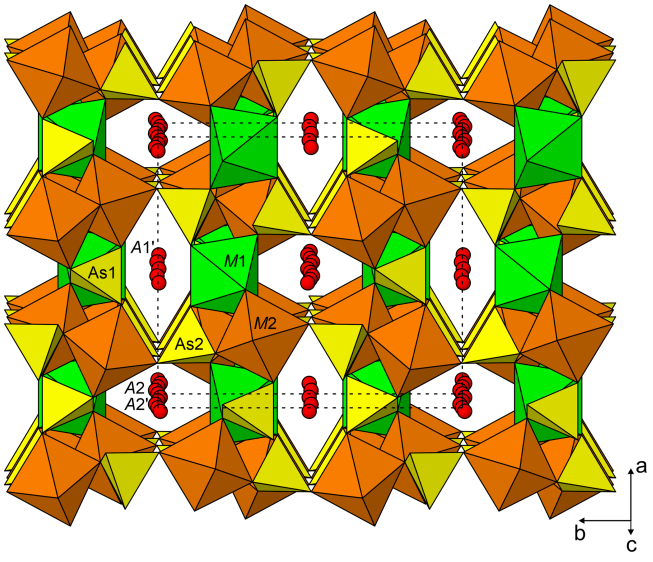

Figure 8. Crystal structure of johanngeorgenstadtite.

7.2 Johanngeorgenstadtite

Johanngeorgenstadtite has the unprotonated alluaudite structure type (Fig. 8); see Hatert (2019). The structure consists of kinked chains of edge-sharing $M1O_6$ and $M2O_6$ octahedra, which are connected by $As1O_4$ and $As2O_4$ tetrahedra to form a framework. The framework contains two types of channels along c: channel one contains three possible cation sites ($A1$, $A1'$ and $A1''$) and channel 2 contains three possible cation sites ($A2$, $A2'$ and $A2''$). In johanngeorgenstadtite, the $M1$, $M2$, $A1'$, $A2$ and $A2'$ sites accommodate Ni^{2+}, Co^{2+} and Cu^{2+}. Because of the strong dominance of Ni indicated by the EPMA ($Ni_{3.56}Co_{0.75}Cu_{0.13}$), the similar scattering powers of Ni, Co and Cu and the similar crystal chemical behaviour of these cations, we assigned Ni to all of the sites and refined the site occupancies. The octahedrally coordinated sites $M1$ and $M2$ refined to similar Ni occupancies, 0.941(9) and 0.943(7), respectively. The $A1'$ channel site refined to full Ni occupancy and the $A2$ and $A2'$ sites refined to partial Ni occupancies, 0.322(13) and 0.464(12), respectively.

The slightly low occupancies for the $M1$ and $M2$ sites suggest that they are essentially fully occupied and are likely to contain some Co, which has a slightly lower scattering power

than Ni; however the closeness of the scattering powers of Ni and Co precluded a joint refinement that would give meaningful quantification of site contents. On the other hand, the BVS sums for the $M1$ and $M2$ sites suggest a preference of Co for the $M1$ site. The $M1$ site BVS is 1.78 vu with occupancy only by Ni and 2.00 vu with only Co, while the $M2$ site BVS is 2.06 vu with only Ni. If all of the 0.75 Co apfu provided by the EPMA were assigned to the $M1$ site, this site would be dominated by Co; however, we do not feel that the BVS alone is sufficient to prove such complete ordering. We think it more likely that Ni is the dominant cation at both sites, with Co somewhat preferring the $M1$ site. The four-coordinated $A1'$ channel site fully occupied by Ni has a very reasonable BVS of 2.03 vu. In unprotonated alluaudite-group arsenates, the larger $A2$ and $A2'$ channel sites normally contain the larger Na^+ cation; however, in the structure of johanngeorgenstadtite, these sites are partially occupied by Ni^{2+}, Co^{2+} and Cu^{2+} and have unusually low BVS values, 1.32 vu for $A2$ and 0.49 vu for $A2'$ (in both cases only based on Ni occupancy).

Data availability. Crystallographic data for both minerals are available in the Supplement.

Supplement. The supplement related to this article is available online at: https://doi.org/10.5194/ejm-32-373-2020-supplement.

Author contributions. ARK identified the minerals as new, conducted powder and single-crystal X-ray diffraction studies and the structure determinations, determined physical and optical properties, recorded Raman spectra, and wrote the paper. BPN conducted the electron probe microanalyses of both niasite and johanngeorgenstadtite. JP interpreted the Raman spectra of niasite and johanngeorgenstadtite. He also provided background on the mining history and geology of the deposit at Johanngeorgenstadt, as well as information on the likely paragenesis of the unusual mineral assemblage that yielded these minerals. JBS recognized niasite as a possible new species, provided the specimen for study and deposition as a cotype, and supplied the information needed to track down its source. MNF provided pieces of the holotype for paganoite and petewilliamsite for study and made additional observations on the entire holotype for these species.

Competing interests. The authors declare that they have no conflict of interest.

Acknowledgements. Michael Rumsey and the anonymous reviewer are thanked for their constructive comments on the manuscript.

Financial support. A portion of this study was funded by the John Jago Trelawney Endowment to the Mineral Sciences Department of the Natural History Museum of Los Angeles County. This research has also been supported by the Czech Ministry of Education, Youth and Sports National sustainability programme I (grant no. LO1603) and the Czech Science Foundation (grant no. GACR 17-09161S).

Review statement. This paper was edited by Edward Grew and reviewed by Mike S. Rumsey and one anonymous referee.

References

Bach, A., Fischer, D., and Jansen, M.: Metastable phase formation of indium monochloride from an amorphous feedstock, Z. Anorg. Allg. Chem., 639, 465–467, 2013.

Barbier, J.: Tetragonal $Ni_{4.35}As_3O_{11.7}(OH)_{0.3}$, Acta Crystallogr., C55, CIF access paper no. IUC9900080, 1999.

Bergemann, C.: Ueber einige Nickelerze, J. Prakt. Chem., 75, 239–244, 1858.

Bufka, A. and Velebil, D.: K dolování uranu v revíru Potůčky v Krušných horách, Bull. Min.-Petr. Odd. NM v Praze, 10, 192–193, 2002.

Davis, R. J., Hey, M. H., and Kingsbury, A. W. G.: Xanthiosite and aerugite, Mineral. Mag., 35, 72–83, 1965.

Dietel, R.: Johanngeorgenstadt – eine Kurzfassung über den Verlauf des Uranerzbergbaues der SAG/SDAG Wismut in den Jahren von 1946 bis 1958, Schriftenreihe des Museums Uranbergbau, Heft 11, Bad Schlema, 2004.

Finger, L. W. and Conrad, P. G.: The crystal structure of "tetragonal almandine-pyrope phase" (TAPP): A reexamination, Am. Mineral., 85, 1804–1807, 2000.

Fischer, D. and Jansen, M.: Low-activation and solid-state syntheses by reducing transport lengths to atomic scales as demonstrated by case studies on $AgNO_3$ and AgO, J. Am. Chem. Soc., 124, 3488–3489, 2002.

Gagné, O. C. and Hawthorne, F. C.: Comprehensive derivation of bond-valence parameters for ion pairs involving oxygen, Acta Crystallogr., B71, 562–578, 2015.

Gopal, R., Rutherford, J. S., and Robertson, B. E.: Closest packing in dense oxides: the structure of a polymorph of $Co_3(AsO_4)_2$, J. Solid State Chem., 32, 29–40, 1980.

Gunter, M. E., Bandli, B. R., Bloss, F. D., Evans, S. H., Su, S. C., and Weaver, R.: Results from a McCrone spindle stage short course, a new version of EXCALIBR, and how to build a spindle stage, Microscope, 52, 23–39, 2004.

Hatert, F.: A new nomenclature scheme for the alluaudite supergroup, Eur. J. Mineral., 31, 807–822, https://doi.org/10.1127/ejm/2019/0031-2874, 2019.

Higashi, T.: ABSCOR, Rigaku Corporation, Tokyo, 2001.

Holleman, A. F., Wiberg, F., and Wiberg, N.: Inorganic Chemistry. Academic Press, San Diego, California, USA, 1–507, 2001.

Krishnamachari, N. T. and Calvo, C.: Magnesium arsenate, $Mg_3As_2O_8$, Acta Crystallogr., B29, 2611–2613, 1973.

Lévy, D. and Barbier, J.: $^{VIII}(Mg,Fe)_{0.85}{}^{VI}(Mg,Fe)_4{}^{IV}(Fe,Ge)_3O_{12}$: a new tetragonal phase and its comparison with garnet, Am. Mineral., 85, 1053–1060, 2000.

Mandarino, J. A.: The Gladstone-Dale relationship – Part IV: The compatibility concept and its application, Can. Mineral., 19, 441–450, 1981.

Murashova, E. V., Velikodnyi, Y. A., and Trunov, V. K.: Crystal structure of $NaMg_4(VO_4)_3$, J. Struct. Chem., 29, 648–650, 1988.

Nestola, F., Burnham, A. D., Peruzzo, L., Tauro, L., Alvaro, M., Walter, M. J., Gunter, M., Anzolini, C., and Kohn, S. C.: Tetragonal Almandine-Pyrope Phase, TAPP: finally a name for it, the new mineral jeffbenite, Mineral. Mag., 80, 1219–1232, 2016.

Ondruš, P., Veselovský, F., Gabašová, A., Hloušek, J., and Šrein, V.: Geology and hydrothermal vein system of the Jáchymov (Joachimsthal) ore district, J. Geosci., 48, 3–18, 2003.

Pouchou, J.-L. and Pichoir, F.: Quantitative analysis of homogeneous or stratified microvolumes applying the model "PAP", in: Electron Probe Quantitation, edited by: Heinrich, K. F. J. and Newbury, D. E. Plenum Press, New York, 31–75, 1991.

Roberts, A. C., Burns, P. C., Gault, R. A., Criddle, A. J., Feinglos, M. N., and Stirling, J. A. R.: Paganoite, $NiBi^{3+}As^{5+}O_5$, a new mineral from Johanngeorgenstadt, Saxony, Germany: description and crystal structure, Eur. J. Mineral., 13, 167–175, https://doi.org/10.1127/0935-1221/01/0013-0167, 2001.

Roberts, A. C., Burns, P. C., Gault, R. A., Criddle, A. J., and Feinglos, M. N.: Petewilliamsite, $(Ni,Co)_{30}(As_2O_7)_{15}$, a new mineral from Johanngeorgenstadt, Saxony, Germany: description and crystal structure, Mineral. Mag., 68, 231–240, 2004.

Sheldrick, G. M.: SHELXT – Integrated space-group and crystal-structure determination, Acta Crystallogr., A71, 3–8, 2015a.

Sheldrick, G. M.: Crystal Structure refinement with SHELX, Acta Crystallogr., C71, 3–8, 2015b.

Vogl, J. F.: Gangverhältnisse und Mineralreichtum Joachimsthals, J. W. Pohlig, Teplitz, 199 pp., 1856.

Weisgerber, G. and Willies, L.: The use of fire in prehistoric and ancient mining – firesetting, Paléorient, 26, 131–149, 2000.